

Archean, highly unradiogenic lead in shallow cratonic mantle

Jun-Bo Zhang¹, Yong-Sheng Liu^{1*}, Mihai N. Ducea^{2,3} and Rong Xu¹¹State Key Laboratory of Geological Processes and Mineral Resources, School of Earth Sciences, China University of Geosciences, Wuhan 430074, China²Department of Geosciences, University of Arizona, Tucson, Arizona 85721, USA³Faculty of Geology and Geophysics, University of Bucharest, 010041 Bucharest, Romania

ABSTRACT

Here, we present coupled geochemical and Sr-Nd-Pb-S isotopic data of Early Cretaceous primitive gabbros from the North China craton. Strikingly, these rocks have highly unradiogenic lead compositions ($^{206}\text{Pb}/^{204}\text{Pb} = 16.58 \pm 0.24$) and anchor one extreme end member (low $^{206}\text{Pb}/^{204}\text{Pb}$ and $^{143}\text{Nd}/^{144}\text{Nd}$) in the global array of oceanic-island volcanics. Our study shows that they originated from an Archean fluid-metasomatized refractory peridotite source, in which highly unradiogenic lead was preferentially released with subducted Archean seawater and sequestered into recrystallized sulfides at shallow mantle depths. Sulfide/silicate partition coefficients for lead show a negative pressure dependence: Lead is more enriched in sulfide with decreasing pressure. Sulfide-bearing and iron-poor harzburgite as well as dunite residues at shallow mantle are expected to develop low U/Pb (and thereby low time-integrated $^{206}\text{Pb}/^{204}\text{Pb}$) relative to a deeper upper-mantle source. Our preferred interpretation is that an Archean, highly unradiogenic lead reservoir may be stored in the spinel-facies refractory cratonic mantle.

INTRODUCTION

The lead (Pb) isotopic composition in Earth's interior is an important parameter that must be accounted for by models that seek to explain the differentiation history of the Earth. The mean continental crust and most oceanic basalts (ocean-island basalt [OIB]; mid-oceanic ridge basalt [MORB]) have apparently higher $^{206}\text{Pb}/^{204}\text{Pb}$ and $^{207}\text{Pb}/^{204}\text{Pb}$ ratios than the bulk silicate earth estimates, and lie either on or immediately to the right of the so-called "meteorite isochron" (Hofmann, 2008). This has been termed the "lead paradox" (Allègre, 1968) and requires the existence of a missing unradiogenic Pb reservoir inside Earth (Hofmann, 2008), which has been argued to have been dissolved in the iron-rich core (Wood and Halliday, 2010) or to reside in the silicate Earth (lower continental crust [Lee et al., 2012; Huang et al., 2014]) or lithospheric mantle (Malaviarachchi et al., 2008; Burton et al., 2012).

Notably, metal-silicate melt partition coefficients for Pb (Lagos et al., 2008) suggest that Pb behaves as a lithophile ($D_{\text{Pb}}^{\text{metal/silicate}} < 1$), implying that the high $^{206}\text{Pb}/^{204}\text{Pb}$ values observed in

OIBs and MORBs cannot be explained easily by high U/Pb ratios in Earth's mantle resulting from Pb pumping to the core (Lagos et al., 2008). Lagos et al. (2008) and Hart and Gaetani (2016) experimentally demonstrated that, as a chalcophile element, Pb is more compatible in sulfide with decreasing pressure (<4.5 GPa; $D_{\text{Pb}}^{\text{sulfide/silicate}} \gg 1$), thus indicating that sulfide is the main host of Pb in sulfide-bearing silicate systematics. U is more incompatible in olivine (ol) and orthopyroxene (opx) than in clinopyroxene (cpx) and garnet (grt; i.e., the main carriers of U in upper mantle; $D_{\text{U}}^{\text{ol/melt}} < D_{\text{U}}^{\text{opx/melt}} < D_{\text{U}}^{\text{grt,cpx/melt}} < 1$; Salters and Longhi, 1999; Parman et al., 2005). Because cpx is preferentially exhausted during melting, U becomes more depleted in cpx-poor peridotite at spinel-facies depths (Parman et al., 2005). Therefore, sulfide-bearing harzburgite/dunite residues at shallow (spinel-facies) mantle depths are expected to be more enriched in Pb but more depleted in U, and thereby retain lower U/Pb. Accordingly, a shallow, early-formed refractory mantle domain will evolve to a relatively low time-integrated $^{206}\text{Pb}/^{204}\text{Pb}$ value.

Furthermore, $D_{\text{Pb}}^{\text{sulfide/silicate}}$ correlates negatively with oxygen fugacity (Lagos et al., 2008),

which implies that Pb becomes more compatible in reduced sulfides ($D_{\text{Pb}}^{\text{sulfide/silicate}} \gg 1$). Therefore, cratonic peridotite could make Pb-rich sulfides survive in the mantle for long periods of time due to its low oxygen fugacity (mean $\Delta\log f_{\text{O}_2} = -2.83$), which is considerably lower than modern oceanic or suprasubduction peridotites (mean $\Delta\log f_{\text{O}_2} = +0.51$; Foley, 2011). If this is true, then a shallow, reduced refractory cratonic mantle that persisted for billions of years is a likely candidate for the highly unradiogenic Pb reservoir.

Here, we present geochemistry and Sr-Nd-Pb-S isotope analyses on the Early Cretaceous Jinan gabbros from within the North China craton (NCC). Our data reveal that Pb excess over U in the shallow cratonic mantle could play a key role in the formation of an unradiogenic Pb reservoir.

GEOLOGICAL SETTING AND SAMPLE DESCRIPTION

The NCC has been divided into the Eastern block, the Western block, and the intervening Trans-North China orogen (Fig. 1A), based on age, lithological assemblage, tectonic evolution, and pressure-temperature-time (*P-T-t*) paths (Zhao et al., 2001). The Eastern block lost its thick lithospheric keel by delamination or thermal erosion (Liu et al., 2008; Zhang et al., 2014). Its extensive magmatic activity and diachronous decratonization started ca. 200 Ma and clustered around 130–120 Ma (Zhang et al., 2014). The Shandong Province is situated in the eastern margin of the NCC (Fig. 1B), where Mesozoic voluminous intrusive and volcanic rocks formed in response to the rapid motion of the Pacific plate (Zhang et al., 2014). The Jinan high-Mg gabbros studied here (127.3 ± 0.7 Ma; Fig. DR1 in the GSA Data Repository¹) were emplaced within the Ordovician marbles in the western Shandong Province. Sulfide (pyrite \pm chalcopyrite)

*E-mail: yshliu@hotmail.com

¹GSA Data Repository item 2020172, analytical methods, Figures DR1 and DR2, and Tables DR1–DR5, is available online at <http://www.geosociety.org/datarepository/2020/>, or on request from editing@geosociety.org.

CITATION: Zhang, J.-B., Liu, Y.-S., Ducea, M.N., and Xu, R., 2020, Archean, highly unradiogenic lead in shallow cratonic mantle: *Geology*, v. 48, p. XXX–XXX, <https://doi.org/10.1130/G47064.1>

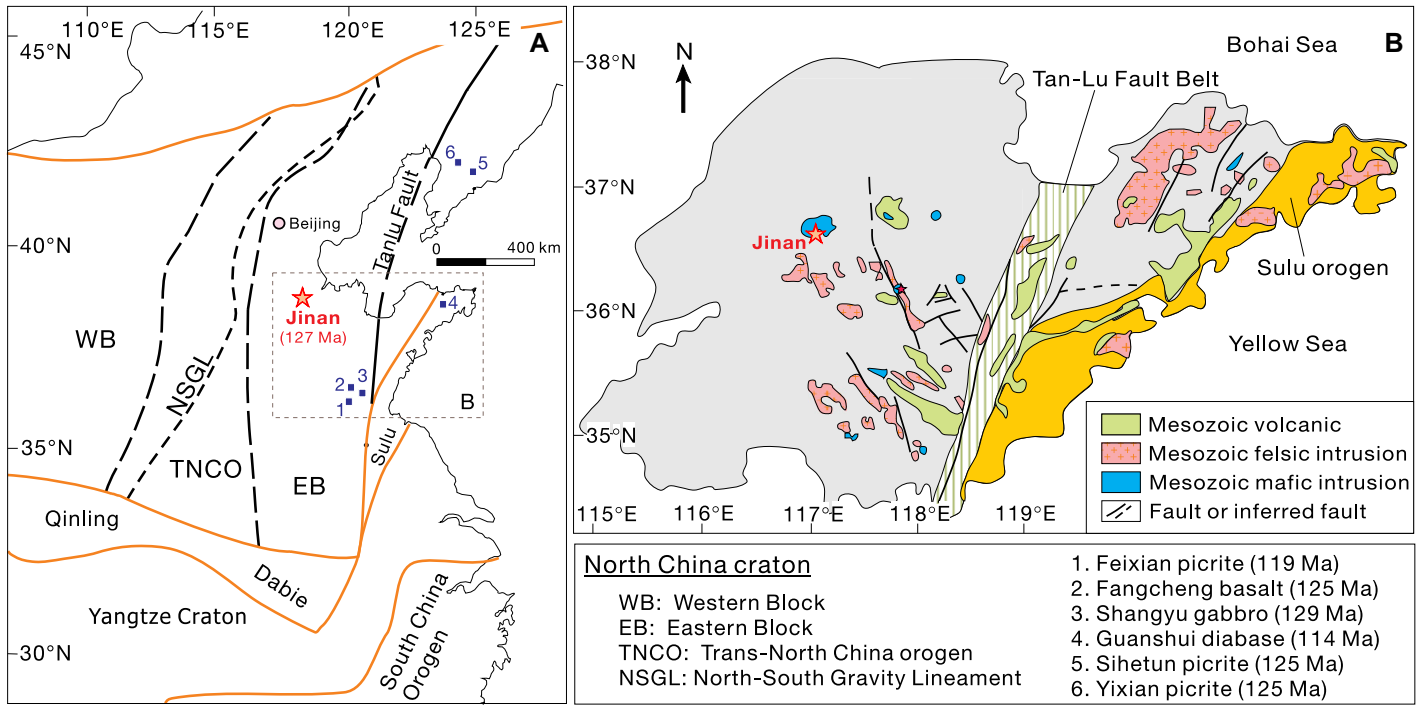


Figure 1. (A) Sketch of Chinese tectonic units (Zhao et al., 2001), showing Jinan gabbro and coeval (129–114 Ma) picritic magmas (North China craton). (B) Simplified geological map of the Shandong region (Zhang et al., 2014).

inclusions are enclosed in olivine and plagioclase crystals, whereas coexisting sulfide and silicate melt inclusions in olivine occur as two separate, immiscible phases (Fig. DR2).

GEOCHEMICAL DATA

Detailed descriptions of the analytical methods and data are summarized in Tables DR1–DR5. The Jinan gabbros have variable SiO₂ (48–

56 wt%), high MgO (up to 13.7 wt%), high Ni and Cr contents (up to 186 and 835 ppm, respectively), and high Mg# (62–69; Table DR2). They display flat to slightly enriched light rare earth (LREE) patterns (La/Yb = 9 ± 3) and are featured by remarkable depletions in Nb and Ta and enrichments in Pb and Ba in the spider diagram (Figs. 2A and 2B). In particular, they have highly unradiogenic Pb isotopic compositions

(²⁰⁶Pb/²⁰⁴Pb = 16.19–16.79, ²⁰⁷Pb/²⁰⁴Pb = 15.15–15.30, ²⁰⁸Pb/²⁰⁴Pb = 36.54–36.62), with relatively evolved Sr and Nd isotopes (⁸⁷Sr/⁸⁶Sr = 0.705–0.706, ε_{Nd} = –14.2 to –9.4; Figs. 3–4). In the global OIB array, the Jinan gabbros display a trend toward the enriched mantle 1 (EM1) component with extremely low ¹⁴³Nd/¹⁴⁴Nd and ²⁰⁶Pb/²⁰⁴Pb values (Fig. 4A). In addition, sulfides separated from the Jinan gabbros show

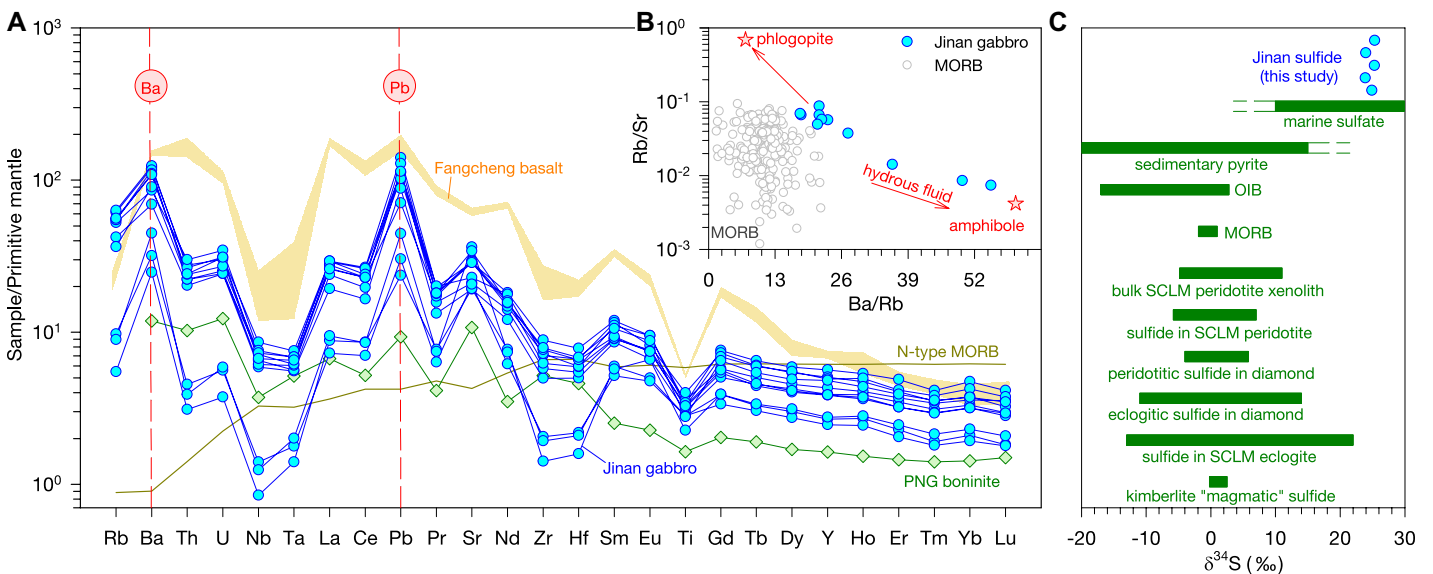


Figure 2. (A) Trace-element patterns, with Papua New Guinea (PNG) boninite (König et al., 2010), normal mid-oceanic ridge basalt (MORB) and primitive mantle (Sun and McDonough, 1989), and Fangcheng basalt (Zhang et al., 2002) for reference. (B) Rb/Sr vs. Ba/Rb with phlogopite and amphibole end members (Zheng et al., 2001). (C) Sulfur isotope ($\delta^{34}\text{S}_{\text{V-CDT}}$ [‰], relative to Vienna Canon Diablo Troilite [V-CDT] reference material) variations in sulfides; also shown are marine sulfate and sedimentary pyrite (Giuliani et al., 2016). OIB—oceanic-island basalt; SCLM—subcontinental lithospheric mantle.

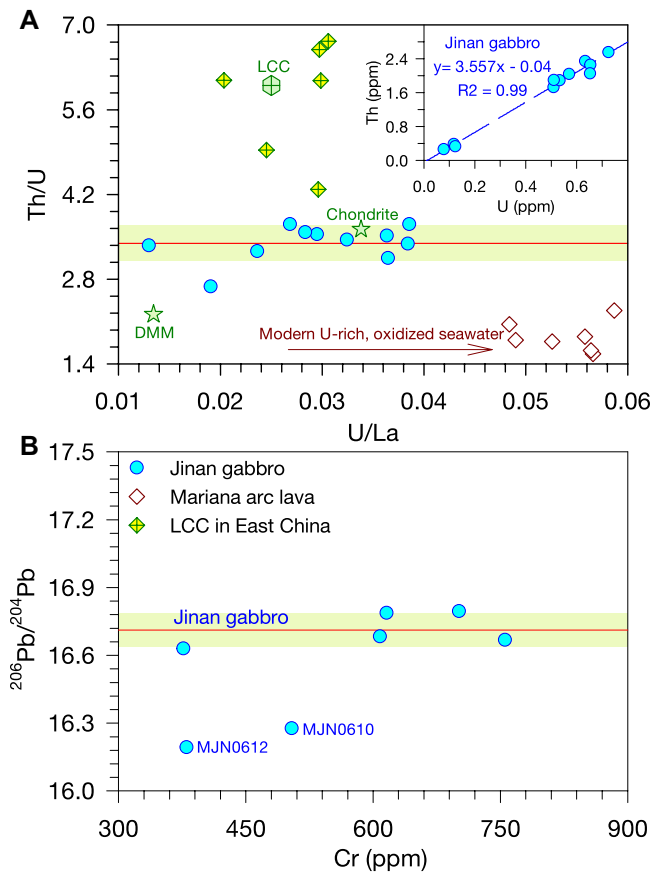


Figure 3. (A) Th/U versus U/La, with chondrite (Sun and McDonough, 1989), depleted mid-oceanic ridge basalt (MORB) mantle (DMM; Workman and Hart, 2005), Mariana arc lava (Elliott et al., 1997), lower continental crust (LCC; Rudnick and Gao, 2014), and LCC in East China (Gao et al., 1998) shown for reference. Inset: Th (ppm) versus U (ppm). (B) Initial ²⁰⁶Pb/²⁰⁴Pb vs. Cr (ppm).

enrichments in heavy sulfur with $\delta^{34}\text{S}_{\text{V-CDT}}$ ranging from +23.9‰ to +25.3‰, where V-CDT indicates the Vienna Canyon Diablo Troilite reference standard (Fig. 2C).

MANTLE DOMAIN WITH HIGHLY UNRADIOGENIC LEAD ISOTOPIC COMPOSITION

Sr-Nd-Pb isotopic ratios of mafic igneous rocks have been used to trace their source features, especially if they are close to primitive values (i.e., have elevated MgO, Ni, and Cr). The most intriguing feature of the Jinan gabbros is their highly unradiogenic Pb isotopic signature ($^{206}\text{Pb}/^{204}\text{Pb} = 16.19\text{--}16.79$), which may balance the high U/Pb mantle exhibited by MORBs and OIBs (Fig. 4A; Hofmann, 2008). The analogous signature in continental basalts from northwestern America was previously ascribed to a contribution from the lower continental crust (LCC; Huang et al., 2014). In that scenario, LCC contamination should have driven the magmatic Th/U ratio toward that of LCC. We note that LCC in different tectonic units in East China shows variable Th/U ratios (4.3–7) higher than the chondritic value of 3.625 (Fig. 3A). However, the Jinan gabbros define an off-LCC, positive trend between Th and U (slope = 3.56; $R^2 = 0.99$) and near-chondritic Th/U ratios (3.4 ± 0.3 ; Fig. 3A), suggesting negligible LCC contamination. Additionally, LCC-derived silicic melts feature low Cr (MgO) contents (Zhang et al., 2014), in contrast to primary basaltic

melt, which is characterized by high MgO and Cr contents. The Jinan gabbros with high Cr (Cr >500 ppm) define a stable $^{206}\text{Pb}/^{204}\text{Pb}$ (or $^{87}\text{Sr}/^{86}\text{Sr}$) value (Figs. 3B and 4A), arguing against LCC contamination. Although Archean sulfide- and plagioclase-rich pyroxenite cumulate may have low U/Pb ratios (and thereby low $^{206}\text{Pb}/^{204}\text{Pb}$), the Jinan gabbros hosting oscillatory zoned magmatic zircons were formed in the Mesozoic (Fig. DR1), implying that their low $^{206}\text{Pb}/^{204}\text{Pb}$ should not have a pyroxenite cumulate origin. As such, the Jinan gabbros most likely originated from a highly unradiogenic Pb mantle domain.

SHALLOW CRATONIC MANTLE: POTENTIAL UNRADIOGENIC LEAD RESERVOIR

Garnet prefers heavy REEs (i.e., Lu) over middle REEs (i.e., Gd; Davies et al., 2015; Zhang et al., 2017). Consequently, basaltic Gd/Lu fractionation could be attributed to a garnet buffer during melting ($D_{\text{Gd/Lu}}^{\text{grt/melt}} < 1$). We note that basaltic Gd/Lu ratios increase with the seismically observed melting depth, as suggested previously (Davies et al., 2015), and that the constant Gd/Lu ratio ($\text{Gd/Lu} = 15 \pm 1$) in the Jinan gabbros is not dependent on Cr content (Fig. 4B). This implies that magmatic Gd/Lu was unaffected by crystal fractionation of ol, cpx, and pl and largely depended on the depth of mantle melting. Note that variable Gd/Lu ratios are present in the NCC high-

Mg basaltic/picritic magmas at 129–114 Ma (Figs. 1A and 4B), which show relatively high Mg# (>65) and have been commonly regarded as indicating similar degrees of melt extraction from the subcontinental lithospheric mantle (SCLM) at different depths (Zhang et al., 2002; Liu et al., 2008). Therefore, their Gd/Lu fractionation was not controlled by the degree of mantle melting. More specifically, there is a clearly positive linear relationship between $^{206}\text{Pb}/^{204}\text{Pb}$ and Gd/Lu ($R^2 = 0.91$) for the Jinan gabbros and NCC high-Mg magmas (Fig. 4B): The highest $^{206}\text{Pb}/^{204}\text{Pb}$ ratios (17.63 ± 0.02) occur in the Feixian picrites with the highest Gd/Lu (49 ± 1), whereas the Jinan gabbros display the lowest $^{206}\text{Pb}/^{204}\text{Pb}$ (16.58 ± 0.24) with the lowest Gd/Lu (15 ± 1), which is close to values ($\text{Gd/Lu} = 10 \pm 2$) of MORBs from the spinel stability field (ol, opx, cpx, and spinel in spinel-facies peridotite could not fractionate Gd from Lu). Hence, the systematic decrease of coeval magmatic $^{206}\text{Pb}/^{204}\text{Pb}$ with decreasing Gd/Lu indicates that the SCLM $^{206}\text{Pb}/^{204}\text{Pb}$ compositions are vertically depth-dependent, and that lower $^{206}\text{Pb}/^{204}\text{Pb}$ values are expected to be preserved in the shallower SCLM.

The Jinan gabbros with high MgO (>13 wt%) and Cr (>500 ppm) contents show minuscule positive Eu anomalies ($\text{Eu}/\text{Eu}^* = 1.03\text{--}1.14$) and moderate Al_2O_3 contents (~11.2 wt%; Table DR2), indicating limited crystal fractionation. These samples have chemical compositions close to the primary melts and thus can be used to trace the features of their mantle source. The Jinan primary melts have apparently negative Nb-Ta anomalies and low K_2O (0.2–0.4 wt%) and LREE contents, and they lack an obvious garnet signature ($\text{La}/\text{Yb} = 9 \pm 3$; $\text{Gd}/\text{Lu} = 15 \pm 1$), partially sharing geochemical affinities with typical boninites extracted from spinel-facies cpx-poor peridotite at subduction zones (Fig. 2A; König et al., 2010). Our observations are opposite to those of continental potassic basalts derived from deep melting of ancient sediments such as K-hollandite (KAlSi_3O_8) in the mantle transition zone, which have extremely high K_2O (>6 wt%) and positive Nb-Ta anomalies (Wang et al., 2017). Furthermore, because olivine favors Fe over Mn ($D_{\text{Fe/Mn}}^{\text{ol/l}} > 1$), low-degree peridotite partial melts may develop low Fe/Mn ratios (Liu et al., 2008). The low Fe/Mn ratios (averaging 57 ± 2 ; Table DR2) of the Jinan gabbros fall in the field of MORBs ($\text{Fe}/\text{Mn} = 55\text{--}58$), implying a refractory mantle source (Liu et al., 2008). Our findings therefore indicate that the source of the Jinan gabbros could be accounted for by the NCC refractory mantle at spinel-facies depth.

The experimental results indicate that $D_{\text{Pb}}^{\text{sulfide/silicate}}$ depends negatively on pressure (Lagos et al., 2008; Hart and Gaetani, 2016), whereas U is more depleted in spinel-facies cpx-poor peridotite (Parman et al., 2005), indicating

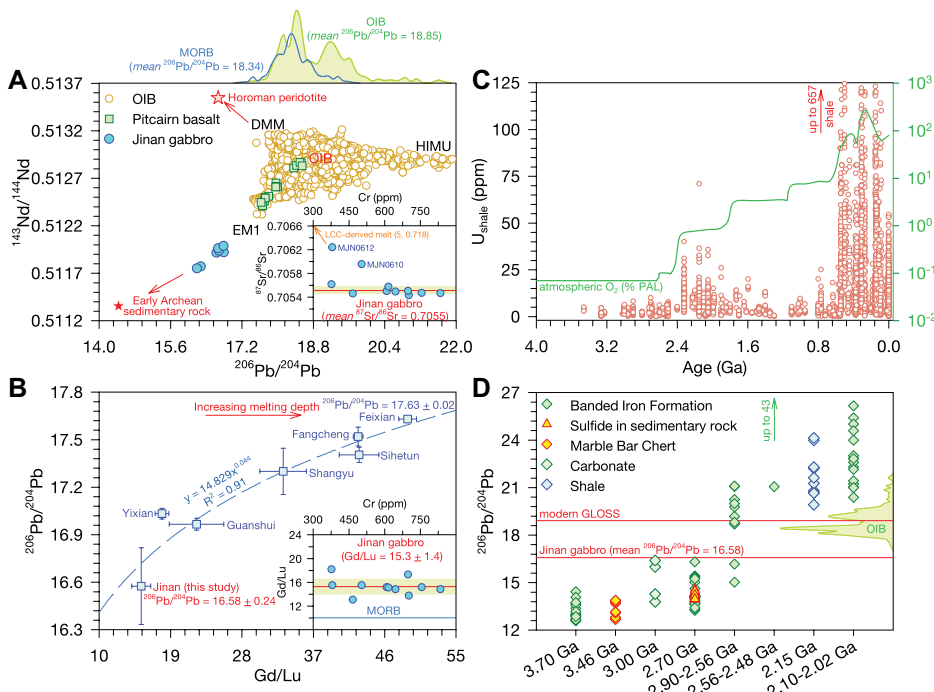


Figure 4. (A) Initial $^{206}\text{Pb}/^{204}\text{Pb}$ versus $^{143}\text{Nd}/^{144}\text{Nd}$, with enriched mantle 1 (EM1); high- μ mantle (HIMU), oceanic-island basalt (OIB; <http://georoc.mpch-mainz.gwdg.de/georoc/>), mid-oceanic ridge basalt (MORB; <http://www.earthchem.org/petdb/>), Pitcairn basalt (Delavault et al., 2016), Early Archean sedimentary rock (Frei and Polat, 2007), Horoman peridotite (Malaviarachchi et al., 2008), and lower continental crust (LCC)—derived melt (Zhang et al., 2014) shown for reference. Inset: Initial $^{87}\text{Sr}/^{86}\text{Sr}$ versus Cr (ppm). (B) Gd/Lu versus $^{206}\text{Pb}/^{204}\text{Pb}$, with Fangcheng basalt (Zhang et al., 2002; Liu et al., 2008); Shangyu gabbro (Yang et al., 2012); Guanshui diabase (Zhang, 2014); and Feixian, Yixian, and Sihetun picrite (Liu et al., 2008; Yang et al., 2012; Geng et al., 2019). Inset: Gd/Lu versus Cr (ppm). (C) Uranium contents (ppm) of black shales and atmospheric oxygen content with time. PAL—present atmospheric level. (D) $^{206}\text{Pb}/^{204}\text{Pb}$ in ca. 3.7–2.02 Ga sedimentary rocks and their hosted sulfides. GLOSS—global subducting sediment. See the Data Repository (see footnote 1) for detailed data sources.

that lower U/Pb could be present in the shallow spinel-facies harzburgite/dunite residues. This is compatible with our observations of highly unradiogenic lead in the shallower SCLM (Fig. 4B), which is generally cold (down to 600 °C, corresponding to 2 GPa; Lee et al., 2011) and reduced (mean $\Delta\log f_{\text{O}_2} = -2.83$; Foley, 2011). We also note that monosulfide solid solution (MSS) is no longer stable at mantle temperatures below 650 °C and decomposes into pyrrhotite, pentlandite, and chalcopyrite (Duran et al., 2019). Because Pb is incompatible in MSS ($D_{\text{Pb}}^{\text{MSS/silicate}} < 1$; Li and Audétat, 2012), the occurrence of highly unradiogenic Pb in the shallow, cold cratonic mantle should be controlled by recrystallized sulfides (Ni-bearing pyrite) rather than by the higher-temperature MSS. At reduced cratonic mantle conditions, Pb is expected to survive in peridotitic sulfides longer (Lagos et al., 2008; Bataleva et al., 2016), and it is also unlikely to partially melt and potentially leave the reservoir, as may be the case for orogenic MSS in the shallow mantle (Ducea and Park, 2000). Consequently, we suggest that a highly unradiogenic Pb reservoir may be hidden in the shallow, cold, reduced, refractory cratonic mantle for billions of years.

ROLE OF ARCHEAN SEDIMENT-DERIVED FLUID IN THE LOW-U/PB MANTLE

The Jinan gabbros are strongly enriched in Ba, with elevated Ba/Rb and Ba/Th ratios (up to 55 and 945, respectively; Fig. 2B), as observed in harzburgitic amphibole (Zheng et al., 2001). This probably reflects hydrous fluid metasomatism in their sources. Dehydration experiments have revealed that Pb is more readily transported by hydrous fluids than U (Kogiso et al., 1997). Depth-dependent U and Pb loss from subducting slabs also shows that Pb is preferentially lost somewhere in the shallow mantle, while U is mostly lost in deeper regions (Kelley et al., 2005). These findings suggest that Pb-bearing fluid percolation into peridotite is more effective at shallower mantle depths. The presence of silicate-sulfide liquid immiscibility (Fig. DR2) reflects substantially elevated S in the Jinan primitive melts sourced from sulfide-rich peridotites. Specifically, our gabbroic sulfides had extremely high $\delta^{34}\text{S}_{\text{V.CDT}}$ values (+23.9‰ to +25.3‰), a feature typical of sedimentary materials (Fig. 2C). These imply that the dehydrated sediments could have

released S-Pb-rich fluids into the Jinan peridotitic sulfides.

Secular U changes in marine shales marked the rapid rise of atmospheric oxygen after the Great Oxidation Event (GOE, ca. 2.4–2.3 Ga; Fig. 4C), which resulted in soluble U^{6+} transport into the oxidized oceans and, ultimately, by means of subduction, back to the mantle (Andersen et al., 2015). Hence, modern arc lavas at subduction zones have systematically subchondritic Th/U (Fig. 3A), indicative of the addition of post-Archean oceanic oxidized U to their sources. Also, $^{206}\text{Pb}/^{204}\text{Pb}$ values of sedimentary rocks and their hosted sulfides record a stepwise shift to higher $^{206}\text{Pb}/^{204}\text{Pb}$ (up to 43) with the onset of the GOE (Fig. 4D). This indicates that Archean sediments deposited in anoxic, U-poor oceans were more enriched in unradiogenic Pb relative to post-Archean sediments deposited in oxidized, U-rich oceans (Figs. 4C and 4D). Moreover, Archean sedimentary rocks show extremely low $^{143}\text{Nd}/^{144}\text{Nd}$ (Fig. 4A) and contain sulfides with mass-independently fractionated sulfur (S-MIF) isotopes (Delavault et al., 2016). So, basalts sampling the Archean sediment-modified mantle are characterized by a positive correlation between extremely low $^{143}\text{Nd}/^{144}\text{Nd}$ and low $^{206}\text{Pb}/^{204}\text{Pb}$, as shown by the Pitcairn basalts hosting S-MIF sulfides and the Jinan gabbros (Figs. 3A and 4A). All these observations suggest that the Jinan mantle source could have been affected by an Archean sediment-derived S- and Pb-rich fluid.

Accordingly, we infer that the early-formed, shallow, refractory mantle source of the Jinan gabbros was overprinted by Archean low-U/Pb fluids, in which S and Pb partitioned into recrystallized sulfides at reduced conditions (Bataleva et al., 2016) to further generate a highly unradiogenic Pb but otherwise enriched mantle domain in the NCC.

ACKNOWLEDGMENTS

This research was supported by the National Natural Science Foundation of China (grants 41530211 and 41503020) and the 111 Project (BP0719022). Ducea acknowledges U.S. National Science Foundation (grant EAR 1725002) and Romanian Executive Agency for Higher Education, Research, Development and Innovation Funding (UEFISCDI) project PN-III-P4-ID-PCCF-2016-0014. We thank Cin-Ty Lee, four anonymous reviewers, and editor Chris Clark for reviews.

REFERENCES CITED

Allègre, C.J., 1968, Comportement des systemes U-Th-Pb dans le manteau superieur et modele d'evolution de ce dernier au cours des temps geologiques: Earth and Planetary Science Letters, v. 5, p. 261–269, [https://doi.org/10.1016/S0012-821X\(68\)80050-0](https://doi.org/10.1016/S0012-821X(68)80050-0).
 Andersen, M.B., Elliott, T., Freymuth, H., Sims, K.W.W., Niu, Y.L., and Kelley, K.A., 2015, The terrestrial uranium isotope cycle: Nature, v. 517, p. 356–359, <https://doi.org/10.1038/nature14062>.
 Bataleva, Y.V., Palyanov, Y.N., Borzdov, Y.M., and Sobolev, N.V., 2016, Sulfidation of silicate mantle by reduced S-bearing metasomatic fluids and

- melts: *Geology*, v. 44, p. 271–274, <https://doi.org/10.1130/G37477.1>.
- Burton, K.W., Cenki-Tok, B., Mokadem, F., Harvey, J., Gannoun, A., Alard, O., and Parkinson, I.J., 2012, Unradiogenic lead in Earth's upper mantle: *Nature Geoscience*, v. 5, p. 570–573, <https://doi.org/10.1038/ngeo1531>.
- Davies, D.R., Rawlinson, N., Iaffaldano, G., and Campbell, I.H., 2015, Lithospheric controls on magma composition along Earth's longest continental hotspot track: *Nature*, v. 525, p. 511–514, <https://doi.org/10.1038/nature14903>.
- Delavault, H., Chauvel, C., Thomassot, E., Devey, C.W., and Dazas, B., 2016, Sulfur and lead isotopic evidence of relic Archean sediments in the Pitcairn mantle plume: *Proceedings of the National Academy of Sciences of the United States of America*, v. 113, p. 12952–12956, <https://doi.org/10.1073/pnas.1523805113>.
- Ducea, M.N., and Park, S.K., 2000, Enhanced mantle conductivity from sulfide minerals, southern Sierra Nevada, California: *Geophysical Research Letters*, v. 27, p. 2405–2408, <https://doi.org/10.1029/2000GL011565>.
- Duran, C.J., Mansur, E.T., and Barnes, S.-J., 2019, Textural and compositional evidence for the formation of pentlandite via peritectic reaction: Implications for the distribution of highly siderophile elements: *Geology*, v. 47, p. 351–354, <https://doi.org/10.1130/G45779.1>.
- Elliott, T., Plank, T., Zindler, A., White, W., and Bourdon, B., 1997, Element transport from slab to volcanic front at the Mariana arc: *Journal of Geophysical Research*, v. 102, p. 14991–15019, <https://doi.org/10.1029/97JB00788>.
- Foley, S.F., 2011, A reappraisal of redox melting in the Earth's mantle as a function of tectonic setting and time: *Journal of Petrology*, v. 52, p. 1363–1391, <https://doi.org/10.1093/ptrology/egg061>.
- Frei, R., and Polat, A., 2007, Source heterogeneity for the major components of 3.7 Ga banded iron formations (Isua Greenstone Belt, western Greenland): Tracing the nature of interacting water masses in BIF formation: *Earth and Planetary Science Letters*, v. 253, p. 266–281, <https://doi.org/10.1016/j.epsl.2006.10.033>.
- Gao, S., Luo, T.C., Zhang, B.R., Zhang, H.F., Han, Y.W., Hu, Y.K., and Zhao, Z.D., 1998, Chemical composition of the continental crust as revealed by studies in east China: *Geochimica et Cosmochimica Acta*, v. 62, p. 1959–1975, [https://doi.org/10.1016/S0016-7037\(98\)00121-5](https://doi.org/10.1016/S0016-7037(98)00121-5).
- Geng, X.L., Foley, S.F., Liu, Y.S., Wang, Z.C., Hu, Z.C., and Zhou, L., 2019, Thermal-chemical conditions of the North China Mesozoic lithospheric mantle and implication for the lithospheric thinning of cratons: *Earth and Planetary Science Letters*, v. 516, p. 1–11, <https://doi.org/10.1016/j.epsl.2019.03.012>.
- Giuliani, A., Fiorentini, M.L., Martin, L.A.J., Farquhar, J., Phillips, D., Griffin, W.L., and LaFlamme, C., 2016, Sulfur isotope composition of metasomatised mantle xenoliths from the Bultfontein kimberlite (Kimberley, South Africa): Contribution from subducted sediments and the effect of sulfide alteration on S isotope systematics: *Earth and Planetary Science Letters*, v. 445, p. 114–124, <https://doi.org/10.1016/j.epsl.2016.04.005>.
- Hart, S.R., and Gaetani, G.A., 2016, Experimental determination of Pb partitioning between sulfide melt and basalt melt as a function of *P*, *T* and *X*: *Geochimica et Cosmochimica Acta*, v. 185, p. 9–20, <https://doi.org/10.1016/j.gca.2016.01.030>.
- Hofmann, A.W., 2008, The enduring lead paradox: *Nature Geoscience*, v. 1, p. 812–813, <https://doi.org/10.1038/ngeo372>.
- Huang, S.C., Lee, C.-T.A., and Yin, Q.-Z., 2014, Missing lead and high ³He/⁴He in ancient sulfides associated with continental crust formation: *Scientific Reports*, v. 4, p. 5314, <https://doi.org/10.1038/srep05314>.
- Kelley, K.A., Plank, T., Farr, L., Ludden, J., and Staudigel, H., 2005, Subduction cycling of U, Th, and Pb: *Earth and Planetary Science Letters*, v. 234, p. 369–383, <https://doi.org/10.1016/j.epsl.2005.03.005>.
- Kogiso, T., Tatsumi, Y., and Nakano, S., 1997, Trace element transport during dehydration processes in the subducted oceanic crust: 1. Experiments and implications for the origin of ocean island basalts: *Earth and Planetary Science Letters*, v. 148, p. 193–205, [https://doi.org/10.1016/S0012-821X\(97\)00018-6](https://doi.org/10.1016/S0012-821X(97)00018-6).
- König, S., Münker, C., Schuth, S., Luguët, A., Hoffmann, J.E., and Kuduon, J., 2010, Boninites as windows into trace element mobility in subduction zones: *Geochimica et Cosmochimica Acta*, v. 74, p. 684–704, <https://doi.org/10.1016/j.gca.2009.10.011>.
- Lagos, M., Ballhaus, C., Munker, C., Wohlgemuth-Ueberwasser, C., Berndt, J., and Kuzmin, D.V., 2008, The Earth's missing lead may not be in the core: *Nature*, v. 456, p. 89–92, <https://doi.org/10.1038/nature07375>.
- Lee, C.-T.A., Luffi, P., and Chin, E.J., 2011, Building and destroying continental mantle: *Annual Review of Earth and Planetary Sciences*, v. 39, p. 59–90, <https://doi.org/10.1146/annurev-earth-040610-133505>.
- Lee, C.-T.A., Luffi, P., Chin, E.J., Bouchet, R., Dasgupta, R., Morton, D.M., Le Roux, V., Yin, Q.Z., and Jin, D., 2012, Copper systematics in arc magmas and implications for crust-mantle differentiation: *Science*, v. 336, p. 64–68, <https://doi.org/10.1126/science.1217313>.
- Li, Y., and Audétat, A., 2012, Partitioning of V, Mn, Co, Ni, Cu, Zn, As, Mo, Ag, Sn, Sb, W, Au, Pb, and Bi between sulfide phases and hydrous basanite melt at upper mantle conditions: *Earth and Planetary Science Letters*, v. 355–356, p. 327–340, <https://doi.org/10.1016/j.epsl.2012.08.008>.
- Liu, Y.S., Gao, S., Kelemen, P.B., and Xu, W.L., 2008, Recycled crust controls contrasting source compositions of Mesozoic and Cenozoic basalts in the North China craton: *Geochimica et Cosmochimica Acta*, v. 72, p. 2349–2376, <https://doi.org/10.1016/j.gca.2008.02.018>.
- Malaviarachi, S.P.K., Makishima, A., Tanimoto, M., Kuritani, T., and Nakamura, E., 2008, Highly unradiogenic lead isotope ratios from the Horoman peridotite in Japan: *Nature Geoscience*, v. 1, p. 859–863, <https://doi.org/10.1038/ngeo363>.
- Parman, S.W., Kurz, M.D., Hart, S.R., and Grove, T.L., 2005, Helium solubility in olivine and implications for high ³He/⁴He in ocean island basalts: *Nature*, v. 437, p. 1140–1143, <https://doi.org/10.1038/nature04215>.
- Rudnick, R.L., and Gao, S., 2014, Composition of the continental crust, in Holland, H.D., and Turekian, K.K., eds., *Treatise on Geochemistry* (2nd ed.): Oxford, UK, Elsevier, p. 1–51, <https://doi.org/10.1016/B978-0-08-095975-7.00301-6>.
- Salter, V.J.M., and Longhi, J., 1999, Trace element partitioning during the initial stages of melting beneath mid-ocean ridges: *Earth and Planetary Science Letters*, v. 166, p. 15–30, [https://doi.org/10.1016/S0012-821X\(98\)00271-4](https://doi.org/10.1016/S0012-821X(98)00271-4).
- Sun, S.S., and McDonough, W.F., 1989, Chemical and isotopic systematics of ocean basalts: Implications for mantle composition and processes, in Saunders, A.D., and Norry, M.J., eds., *Magma-tism in the Ocean Basins*: Geological Society [London] Special Publication 42, p. 313–345, <https://doi.org/10.1144/GSL.SP.1989.042.01.19>.
- Wang, X.-J., Chen, L.-H., Hofmann, A.W., Mao, F.-G., Liu, J.-Q., Zhong, Y., Xie, L.-W., and Yang, Y.-H., 2017, Mantle transition zone-derived EM1 component beneath NE China: Geochemical evidence from Cenozoic potassic basalts: *Earth and Planetary Science Letters*, v. 465, p. 16–28, <https://doi.org/10.1016/j.epsl.2017.02.028>.
- Wood, B.J., and Halliday, A.N., 2010, The lead isotopic age of the Earth can be explained by core formation alone: *Nature*, v. 465, p. 767–770, <https://doi.org/10.1038/nature09072>.
- Workman, R.K., and Hart, S.R., 2005, Major and trace element composition of the depleted MORB mantle (DMM): *Earth and Planetary Science Letters*, v. 231, p. 53–72, <https://doi.org/10.1016/j.epsl.2004.12.005>.
- Yang, D.B., Xu, W.L., Pei, F.P., Yang, C.H., and Wang, Q.H., 2012, Spatial extent of the influence of the deeply subducted South China block on the southeastern North China block: Constraints from Sr-Nd-Pb isotopes in Mesozoic mafic igneous rocks: *Lithos*, v. 136–139, p. 246–260, <https://doi.org/10.1016/j.lithos.2011.06.004>.
- Zhang, H.F., Sun, M., Zhou, X.H., Fan, W.M., Zhai, M.G., and Yin, J.F., 2002, Mesozoic lithosphere destruction beneath the North China craton: Evidence from major-, trace-element and Sr-Nd-Pb isotope studies of Fangcheng basalts: *Contributions to Mineralogy and Petrology*, v. 144, p. 241–254, <https://doi.org/10.1007/s00410-002-0395-0>.
- Zhang, J.B., 2014, Recycled Lower Continental Crust in the North China Craton: Evidence from Mesozoic/Cenozoic Magmatism in Shandong [Ph.D. thesis]: Wuhan, China, China University of Geosciences, 137 p.
- Zhang, J.B., Ling, W.L., Liu, Y.S., Duan, R.C., Gao, S., Wu, Y.B., Yang, H.M., Qiu, X.F., and Zhang, Y.Q., 2014, Episodic Mesozoic thickening and reworking of the North China Archean lower crust correlated to the fast-spreading Pacific plate: *Journal of Asian Earth Sciences*, v. 80, p. 63–74, <https://doi.org/10.1016/j.jseaes.2013.10.031>.
- Zhang, J.B., Liu, Y.S., Ling, W.L., and Gao, S., 2017, Pressure-dependent compatibility of iron in garnet: Insights into the origin of ferroperitic melt: *Geochimica et Cosmochimica Acta*, v. 197, p. 356–377, <https://doi.org/10.1016/j.gca.2016.10.047>.
- Zhao, G.C., Wilde, S.A., Cawood, P.A., and Sun, M., 2001, Archean blocks and their boundaries in the North China craton: Lithological, geochemical, structural and *P-T* path constraints and tectonic evolution: *Precambrian Research*, v. 107, p. 45–73, [https://doi.org/10.1016/S0301-9268\(00\)00154-6](https://doi.org/10.1016/S0301-9268(00)00154-6).
- Zheng, J.P., O'Reilly, S.Y., Griffin, W.L., Lu, F., Zhang, M., and Pearson, N.J., 2001, Relict refractory mantle beneath the eastern North China block: Significance for lithosphere evolution: *Lithos*, v. 57, p. 43–66, [https://doi.org/10.1016/S0024-4937\(00\)00073-6](https://doi.org/10.1016/S0024-4937(00)00073-6).

Printed in USA